Temperature, composition and molecular-weight dependence of the binary interaction parameter of polystyrene/poly(vinyl methyl ether) blends

Charles C. Han, Barry J. Bauer, John C. Clark, Yoshio Muroga*, Yushu Matsushita*, Mamoru Okada†, Qui Tran-cong‡ and Taihyun Chang§

Polymers Division, Institute for Materials Science and Engineering, National Bureau of Standards, Gaithersburg, MD 20899, USA

and Isaac C. Sanchez

Alcoa Laboratories, Alcoa Centre, PA 15069, USA

(Received 1 April 1988; accepted 4 April 1988)

The binary interaction parameter χ_{eff} has been obtained for deuterated polystyrene/poly(vinyl methyl ether) blends as a function of temperature, composition and molecular weight from small-angle neutron scattering experiments. The consistency of the correlation length ξ, the zero-wavenumber scattering intensity $S(0)$ and the χ_{eff} parameter with the mean-field prediction has been demonstrated by the q dependence of the static structure factor $S(q)$ and the $1/T$ dependence of ξ^{-2}, $S(0)^{-1}$ and χ_{eff}. The effective interaction parameter χ_{eff} can be related to the Flory–Huggins interaction parameter χ_F. The free-energy function as well as the spinodal curve and cloud-point curve have been constructed.

(Keywords: interaction parameter; polystyrene; poly(vinyl methyl ether); blends)

INTRODUCTION

The technical importance of polymer blends has been well recognized in recent years[1]. Making polymers miscible through chemical structure modification is a very important topic, but miscibility may not be the ultimate characteristic one is looking for. This is because synergistic effects which enhance the property of a phase-separated material mainly come from molecular alignment, reinforcement, phase domain size and morphology.

In order to understand and possibly control the domain sizes and morphology due to phase decomposition, one has to understand thermodynamics (statics) as well as phase-separation kinetics (dynamics). We understand that statics and dynamics are inseparable subjects if we wish to talk about phase behaviour of even a simple binary system. The most important quantity needed in both static and dynamic characterization is the free energy (of mixing) of the system as a function of temperature and composition. For the case of polymer systems, we also need to know the molecular-weight dependence of the free-energy function.

Small-angle neutron scattering (SANS) has been used[2-4] to measure the effective or scattering binary interaction parameter χ_{eff} (for convenience, we will drop the subscript 'effective' or 'scattering' throughout this paper and define $\chi_{eff}=\chi_{scatt}=\chi$) for a deuterated polystyrene/poly(vinyl methyl ether) (PSD/PVME) system. This technique offers a rather simple, fast and accurate method of obtaining the χ parameter. Therefore, a systematic study of this χ parameter as a function of composition (ϕ), temperature (T) and molecular weight (MW) is possible.

The extraction of the χ parameter from SANS measurements depends on the mean-field nature of the polymer system and the random-phase approximation (RPA) calculation. Nevertheless, within our measurement error, we have found this procedure quite satisfactory. Furthermore, we should point out that the χ parameter extracted from this procedure is different from the χ_F parameter in the Flory–Huggins free-energy function as long as the χ_F parameter is allowed to be compositionally dependent. The exact origin of this compositional dependence of χ_F is not certain. It could be caused by residual entropic effects of monomer size difference between the two components, by the local packing orientations, by the chain-end effect, etc.[5-8]. We shall discuss the relationship between χ, which is measured in our experiment, and χ_F, which is used in the free-energy function of Flory–Huggins type later. We should point out that we have allowed the χ_F to be compositionally dependent, which is different from the original definition of the Flory–Huggins χ parameter. Essentially, we have incorporated all residual compositional dependence into χ_F. But, as long as the interaction between the two types of monomer can be described by a single q-independent potential function $U(\phi,T)$ at a given ϕ and T, the RPA calculation will provide a general scattering factor $S(q)$, which allows the extraction of the effective interaction parameter χ from

* Current address: Department of Synthetic Chemistry, Nagoya University, Nagoya 464, Japan
† Current address: Department of Polymer Chemistry, Tokyo Institute of Technology, Tokyo 152, Japan
‡ Current address: Department of Polymer Science and Engineering, Kyoto Institute of Technology, Kyoto 606, Japan
§ Current address: Korean Research Institute for Chemical Technology, Chungnam, Korea

0032-3861/88/112002-13$03.00

the scattering experiment. Then, through the compositional dependence of χ, the free-energy function can be constructed according to the calculation by Sanchez[9], which will be demonstrated later.

In this paper, we present a systematic study of the effective χ parameter as a function of ϕ, T and MW for high-molecular-weight and narrow-molecular-weight-distribution deuterated polystyrene/poly(vinyl methyl ether) systems by the SANS technique. The free-energy function has then been constructed numerically from these measurements.

THEORETICAL BACKGROUND

It has been shown by de Gennes[10] and later by Binder[11] that for a non-interacting polymer system, the random-phase approximation calculation gives an inverse additivity of the scattering structure factor $S(q)$. In other words, the inverse of the total scattering structure factor $S(q)$ equals the sum of the inverse of the individual structure factor $S_A(q)$ and $S_B(q)$ for a binary polymer system:

$$\frac{1}{S(q)}=\frac{1}{N_A\phi_A S_A(q)}+\frac{1}{N_B\phi_B S_B(q)} \tag{1}$$

On the other hand, for an interacting system with a mean-field potential U, the total structure factor can be represented as:

$$\frac{1}{S(q)}=\frac{1}{N_A\phi_A S_A(q)}+\frac{1}{N_B\phi_B S_B(q)}-2\chi \tag{2}$$

By putting in the scattering lengths and other constants, equation (2) can be written as[4]:

$$\frac{k_N}{S(q)}=\frac{1}{\phi_A N_A v_A S_D(U_A)}+\frac{1}{\phi_B N_B v_B S_D(U_B)}-\frac{2\chi}{v_0} \tag{3}$$

where

$$k_N=N_0\left(\frac{a_A}{v_A}-\frac{a_B}{v_B}\right)^2$$

with N_0 being the Avogadro number, a_i being the scattering length per mole of monomer i, v_0 and v_i being the molar volumes of a reference unit cell and of the ith segment respectively. The single-chain structure factor $S_D(U_i)$ may be represented by the Debye function:

$$S_D(U_i)=\frac{2}{U_i^2}[\exp(-U_i)-1+U_i] \tag{4}$$

with $U_i=q^2R_{gi}^2/3$ and q is the magnitude of the scattering wavevector:

$$q\equiv|\mathbf{q}|=(4\pi/\lambda)\sin(\theta/2)$$

λ is the wavelength of the incident beam and θ is the scattering angle. R_{g_i}, N_i and ϕ_i are the radius of gyration, the degree of polymerization and the volume fraction of polymer i, respectively. The χ parameter obtained is related to the mean-field potential U for a given composition and temperature as:

$$U=v_A v_B\chi/v_0^2 \tag{5}$$

By the expansion of the Debye function and dropping all terms higher than the second moment, equation (3) can be written in the Ornstein–Zernike form:

$$S(q)=S(q=0)/[1+\xi^2(T,\phi)q^2] \tag{6}$$

with

$$\xi^2(T,\phi)=\frac{\overline{b^2}}{36}[\phi_A\phi_B(\chi_s-\chi)]^{-1} \tag{7}$$

and

$$\frac{\overline{b^2}}{v_0}=\phi_A\phi_B\left(\frac{b_A^2}{v_A\phi_A}+\frac{b_B^2}{v_B\phi_B}\right) \tag{8}$$

where $\xi(T,\phi)$ is the correlation length at temperature T and composition $\phi=\phi_A$, b_i is the statistical segment length of the ith component and χ_s is the effective χ parameter at the spinodal point:

$$\frac{\chi_s}{v_0}=\frac{1}{2}\left(\frac{1}{v_A\phi_A N_A}+\frac{1}{v_B\phi_B N_B}\right) \tag{9}$$

In the vicinity of the phase separation temperature, both $S(q=T,\phi)$ and $\xi(T,\phi)$ may have scaling forms as often observed in critical fluctuation phenomena:

$$S(q=0,T,\phi)=S_0(\phi)\varepsilon^{-\gamma} \tag{10}$$

$$\xi(T,\phi)=\xi_0(\phi)\varepsilon^{-\nu} \tag{11}$$

where

$$\varepsilon=\left|\frac{T-T_c}{T_c}\right| \tag{12}$$

If a binary polymer system can be described by the mean-field model[12,13], then ν and γ should have values of 1/2 and 1 respectively. One should notice that χ has a unit of energy per k_BT; the $1/T$ dependence of χ together with equations (3) and (7) predict that in the vicinity of the critical temperature T_c:

$$S(0,T,\phi)\propto|T-T_c|^{-1} \tag{13}$$

and

$$\xi(\phi)\propto|T-T_c|^{-1/2} \tag{14}$$

These are consistent with the mean-field exponents of ν and γ. However, this is a result which should be expected because the RPA calculation itself is a mean-field calculation. Therefore, a check on the $1/T$ dependence of χ or a check on equations (13) and (14) are equivalent to a check on the mean-field exponents ν and γ. We shall discuss this point again in the discussion section.

EXPERIMENTAL

Materials

Poly(styrene-d_8) (PSD) was prepared by anionic polymerization of styrene-d_8 in benzene with

Table 1 Molecular weight and polydispersity of the three series of samples used for SANS study

	PSD		PVME	
	M_w	M_w/M_n	M_w	M_w/M_n
L series	230×10^3	1.14	389×10^3	1.25
M series	402×10^3	1.42	210×10^3	1.32
H series	593×10^3	1.48	1100×10^3	1.26

butyllithium as initiator using standard techniques[14]. The molecular-weight distribution was measured by gel permeation chromatography (g.p.c.) and the molecular weights and polydispersities are listed in *Table 1*.

Poly(vinyl methyl ether) (PVME) was polymerized by cationic polymerization of vinyl methyl ether in toluene with boron trifluoride–ethyl ether complex as an initiator[15]. The polymer was fractionated with toluene as a solvent and heptane as a non-solvent. The fractions used in this study are also listed in *Table 1*. The weight-average molecular weight and polydispersities were measured by g.p.c.

Sample preparation

The neutron scattering samples were prepared by solution casting from toluene. In the blends designated the M series, no antioxidant was used. But, in the L and H series, 0.05 wt% of Santonox R* (Monsanto Chemical Company) was added as antioxidant. The cast films were cut and compression moulded at 120°C into circular specimens. The thickness of all specimens was 1.6 mm, with a diameter of 19 mm. All specimens were then thoroughly dried in a vacuum at 120°C for at least 16 h and sandwiched between oxygen-free Cu windows for SANS measurements. All SANS measurements were carried out at the temperature reported in this paper. No quenched samples have been used, in order to avoid any possible artefacts caused by quenching. All samples were kept in vacuum at 100°C between measurements to ensure their dryness.

Small-angle neutron scattering experiments

SANS experiments were carried out at the National Bureau of Standards Research Reactor. The wavelength λ of the incident beam was monochromatized to 6 Å by a velocity selector. A focusing collimation was used which gives a minimum scattering wavevector q_{min} of 6×10^{-3} Å^{-1}. The observed scattering intensity at a given temperature, molecular-weight combination and composition was corrected for electronic noise, background radiation and detector inhomogeneity. It is then normalized against a dry silica gel which serves as a secondary standard[16], to give the absolute intensity. Finally, it is circularly averaged to give the q, ϕ and T dependence of the scattering structure factor $S(q)$.

RESULTS AND DISCUSSION

Small-angle neutron scattering measurements have been carried out for all three series of molecular-weight combinations at various temperatures and concentrations listed in *Table 1* and Appendix 2. The experimental structure factor $S(q)$ was fitted to equation (3) with a non-linear least-squares regression program. Since the first two terms, which include the inverse of the structure factors $S_D(U_A)^{-1}$ and $S_D(U_B)^{-1}$, are highly correlated, it is impossible to treat the statistical segment length b of PSD and PVME as two independent fitting parameters. Therefore, we have used a single averaged parameter, b^2_{ave} in the fitting procedure, with[4]:

$$U_i=\frac{N_i v_i}{6}\left(\frac{b^2_{ave}}{v_0}\right)q^2 \qquad (15)$$

In *Figure 1*, the scattering intensity $S(q)$ is displayed vs. q for the 30/70 sample of the M series at various temperatures as shown in the figure. Full curves are best fits according to equation (3). Three parameters, i.e. b^2_{ave}, χ/v_0 and a baseline factor, were used in all regression analyses. The baseline factor was introduced for possible incorrect subtraction of incoherent scattering. It is always very small for all experiments reported in this paper. $S(q=0,\phi,T)$, $\xi(\phi,T)$, $\chi(\phi,T)/v_0$ and b^2_{ave} obtained from the fitting and equations (3) and (7) are listed in Appendix 1. The molar volumes of 100.54 cm^3 mol^{-1} and 55.47 cm^3 mol^{-1} are used for PSD and PVME repeat units respectively. In *Figure 2*, reciprocal square correlation length (ξ^{-2}) is plotted vs. T for various compositions for the H series results. The ξ^{-2} values can be represented by a straight line near the spinodal temperature which is the intercept at $\xi^{-2}=0$ as shown in the figure. This is equivalent to a log ξ vs. log ε plot with an exponent of $\nu=1/2$ as indicated by equations (11) and (14). A similar plot of $S(q=0)^{-1}$ vs. T is shown in *Figure 3*. Again, a good straight-line representation of the data is obtained near T_s which indicates that the mean-field exponent of $\nu=1$ is consistent with the results. Notice that similar behaviour can be observed for the critical composition ($\phi_{PSD}=0.2$) as well as off-critical compositions.

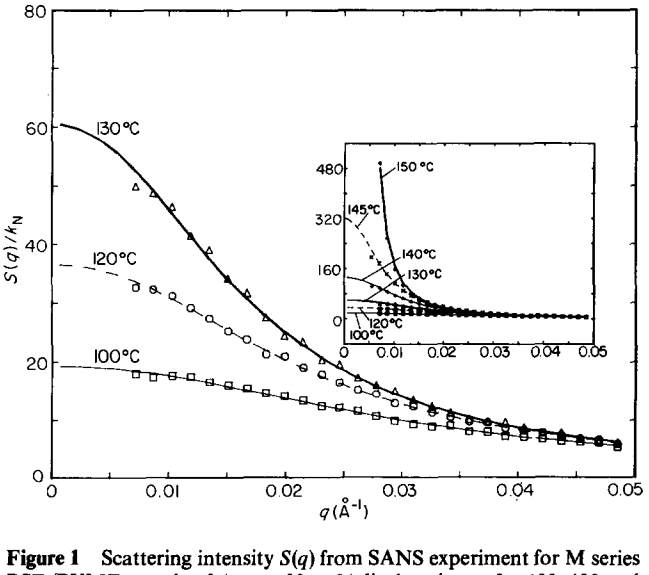

Figure 1 Scattering intensity $S(q)$ from SANS experiment for M series PSD/PVME sample of $\phi_{PSD}=30$ wt% displayed vs. q for 100, 120 and 130°C. Full or broken curves are best fits according to equation (3). Experiments with several other temperatures are displayed at reduced scale in the insert

* *Disclaimer*. Certain commercial materials and instruments are identified in this paper in order to specify the experimental procedure. In no case does such identification imply recommendation or endorsement by the National Bureau of Standards

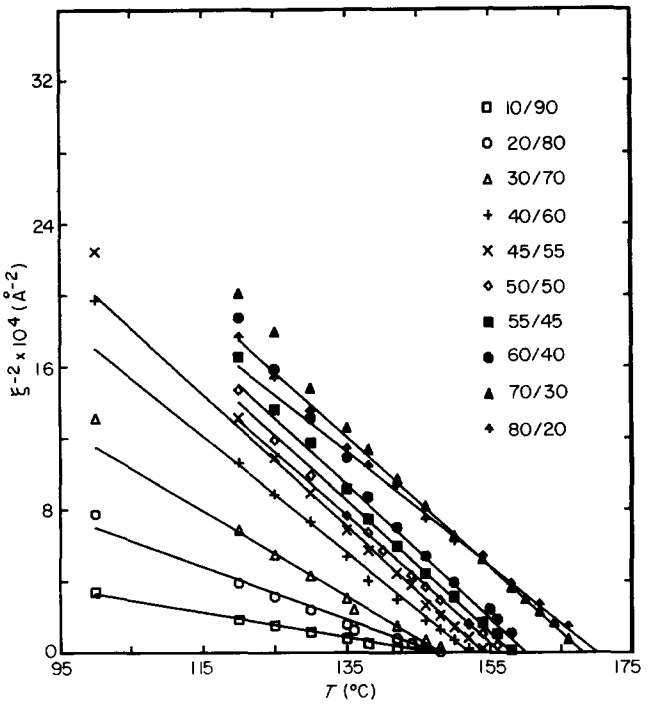

Figure 2 Reciprocal square correlation length ξ^{-2} plotted vs. T for various compositions for H series sample

In *Figure 4*, χ/v_0 values are plotted against $1/T$ for the H series sample at various compositions as indicated in the figure. At any given composition, the χ/v_0 values follow the $1/T$ dependence as is clearly indicated by the straight lines in this figure. As mentioned before, this is necessary in order to obtain the mean-field exponents from equations (3) and (7). Substituting χ by $B+A/T$ into equations (3) and (7) we obtain:

$$k_N S(q=0)^{-1} = \frac{2\chi_s}{v_0} - \frac{2\chi}{v_0} = \frac{2A}{v_0}\left(\frac{1}{T} - \frac{1}{T_s}\right) = \frac{2A}{v_0}\frac{T_s - T}{TT_s} \quad (16)$$

$$\xi^{-2} = \frac{A36\phi_A\phi_B}{T_0^2}\left(\frac{1}{T} - \frac{1}{T_s}\right) = \frac{A36\phi_A\phi_B}{\bar{b}^2}\left(\frac{T_s - T}{TT_s}\right) \quad (17)$$

Equations (16) and (17) indicate that at $T \ll T_s$, ξ^{-2} and $S(q=0)^{-1}$ should have higher values than a strict ΔT prediction indicated in equations (13) and (14). If we examine the ξ^{-2} and $S(0)^{-1}$ data carefully in *Figures 2* and *3*, positive deviation is always found at $T \ll T_s$. This indicates that the RPA may be a very good model for concentration fluctuations for any composition and temperature even at temperatures far away from T_s. A better procedure to examine a polymer/polymer system is to fit the $S(q)$ data to the RPA calculation of equation (3) and to examine the reciprocal temperature dependence of χ/v_0, ξ^{-2} and $S(0)^{-1}$ consistently for a wide range of temperatures and compositions. It is dangerous to interpret the small positive curvature from either the $S^{-1}(0)$ vs. T plot or from the ξ^{-2} vs. T plot as a crossover from mean-field to Ising prediction[17]. The same data from *Figure 2* are replotted as ξ^{-2} vs. $1/T$ in *Figure 5* to demonstrate this point. Similar plots for $S(0)^{-1}$ vs. $1/T$ for all three molecular-weight samples have been carried out as well. Spinodal temperatures have been obtained consistently from the intercepts of ξ^{-2} and $S(0)^{-1}$ going to zero and are listed in Appendix 2.

The χ/v_0 values for 30 wt% and 50 wt% samples of all three molecular-weight series are plotted against $1/T$ in *Figure 6* together with least-squares fitted lines through each set of data. The same kind of comparison can be made for other concentrations as well. In general, we do not see significant molecular-weight dependence. The concentration dependence of χ/v_0 at 130°C is displayed in *Figure 7*. It seems that χ/v_0 varies linearly with composition except that there may be a very small curvature at $\phi_{PSD} < 0.3$. If the free energy of mixing of a

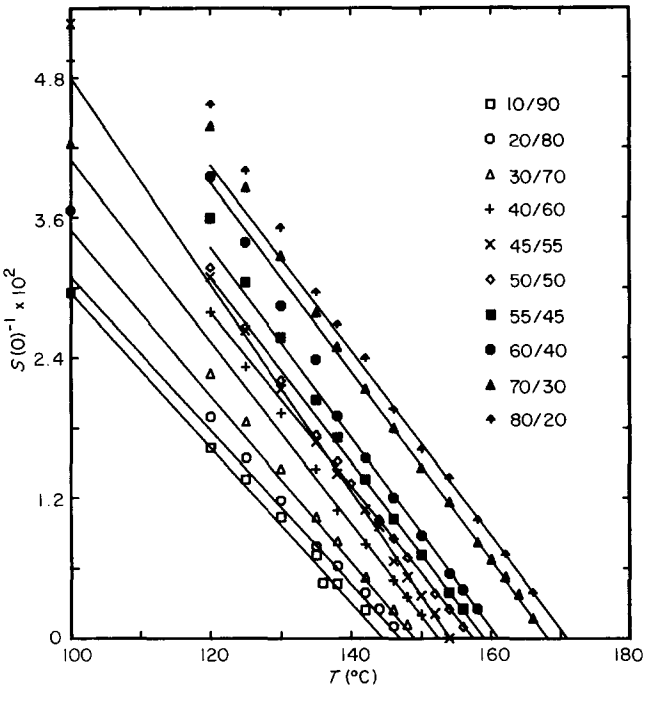

Figure 3 $S(0)^{-1}$ plotted vs. T for the H series sample

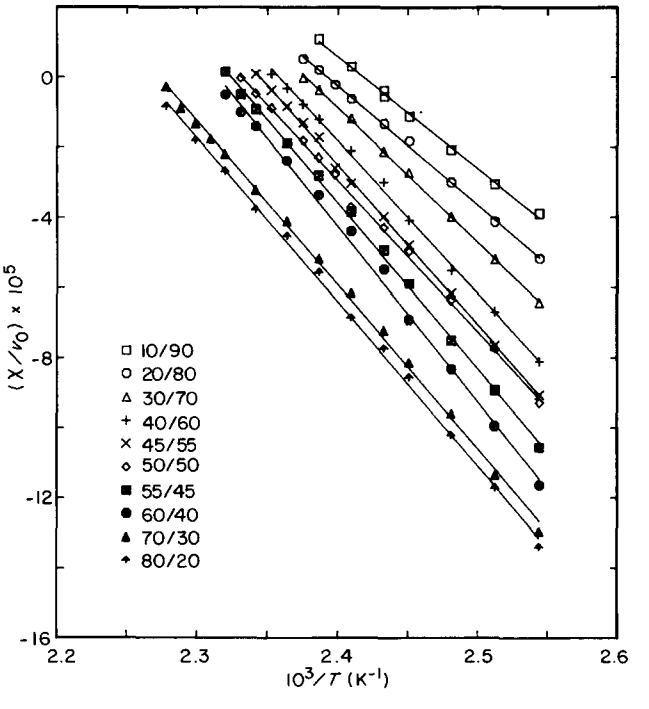

Figure 4 Reciprocal temperature dependence of χ/v_0 for various compositions of the H series sample

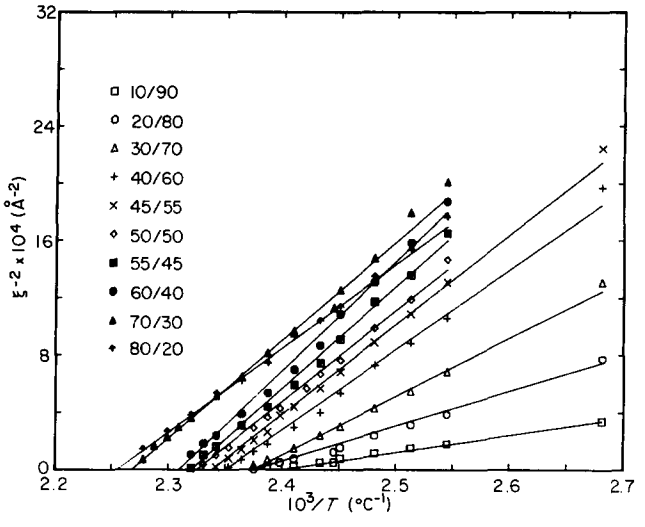

Figure 5 Reciprocal square correlation length plotted vs. $1/T$ for various compositions for the H series sample

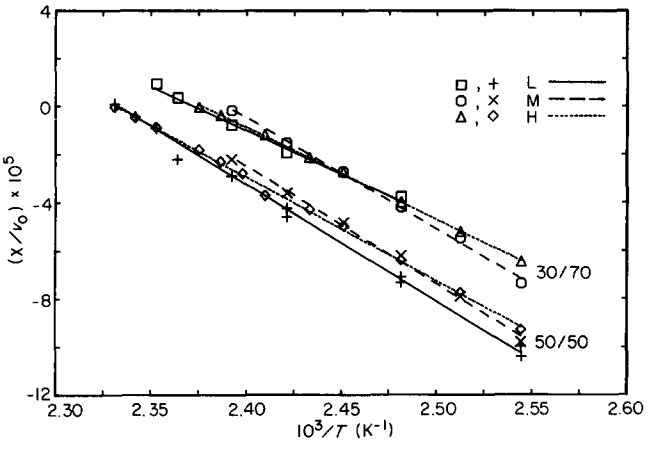

Figure 6 Interaction parameter χ/v_0 vs. $1/T$ for H, M and L series of samples, together with linear least-square fitted lines. The upper group are data at 30/70 composition while the lower group are data at 50/50 composition

binary polymer system follows a Flory–Huggins type[18] as:

$$f \equiv \Delta F/v_0 \equiv \Delta f = \Delta f_{comb} + \Delta f_{ex}$$
$$= k_B T\left(\frac{\phi \ln \phi}{N_A v_A} + \frac{(1-\phi)\ln(1-\phi)}{N_B v_B} + \frac{\phi(1-\phi)\chi_F}{v_0}\right) \quad (18)$$

with the interaction parameter χ_F as a function of both composition and temperature ($1/T$ dependence) and v_i as the monomer volume of the ith component, then the spinodal and critical point can be easily obtained[19] at $(\partial^2 f/\partial^2\phi)=0$ and $(\partial^3 f/\partial\phi^3)=0$. Since the scattering structure factor at $q=0$ is inversely proportional to $\partial^2 f/\partial\phi^2$, we can rewrite equation (3) as:

$$\left.\frac{k_N}{S(q)}\right|_{q=0} = \frac{1}{v_0}\frac{1}{RT}\frac{\partial^2(\Delta F)}{\partial\phi^2} = \frac{1}{k_B T}\left(\frac{\partial^2 f}{\partial\phi^2}\right)$$
$$= \frac{1}{v_A\phi_A N_A} + \frac{1}{v_B\phi_B N_B} - \frac{2\chi}{v_0} \quad (19)$$

or

$$\frac{\partial^2 f}{\partial\phi^2} = \frac{2}{v_0}(\chi_s - \chi) \quad (20)$$

By letting $N_A v_A = v_1$, $N_B v_B = v_2$ and $v_0 = 1$ for simplicity, equation (18) can be rewritten as:

$$f = k_B T[(\phi_1/v_1)\ln\phi_1 + (\phi_2/v_2)\ln\phi_2 + \phi_1\phi_2\chi_F] \quad (21)$$

Following the calculation of Sanchez[9], it can be shown that

$$\chi_F = \phi_2\chi_{\mu 1} + \phi_1\chi_{\mu 2} \quad (22)$$

with

$$k_B T\phi_2^2\chi_{\mu 1} \equiv \Delta f_{ex} + \phi_2 \mathrm{d}(\Delta f_{ex})/\mathrm{d}\phi_1$$
$$k_B T\phi_1^2\chi_{\mu 2} \equiv \Delta f_{ex} + \phi_1 \mathrm{d}(\Delta f_{ex})/\mathrm{d}\phi_2 \quad (23)$$

and

$$\chi_{\mu 1} = (2/\phi_2^2)\int_0^{\phi_2} \phi_2'\chi \,\mathrm{d}\phi_2'$$
$$\chi_{\mu 2} = (2/\phi_1^2)\int_0^{\phi_1} \phi_1'\chi \,\mathrm{d}\phi_1' \quad (24)$$

Since we have χ values for various compositions and temperatures, it is clear that the free energy of mixing can be constructed from equations (24), (22) and (21). We try to correlate χ/v_0 values by empirical functions before the construction of the free-energy function. We have tried

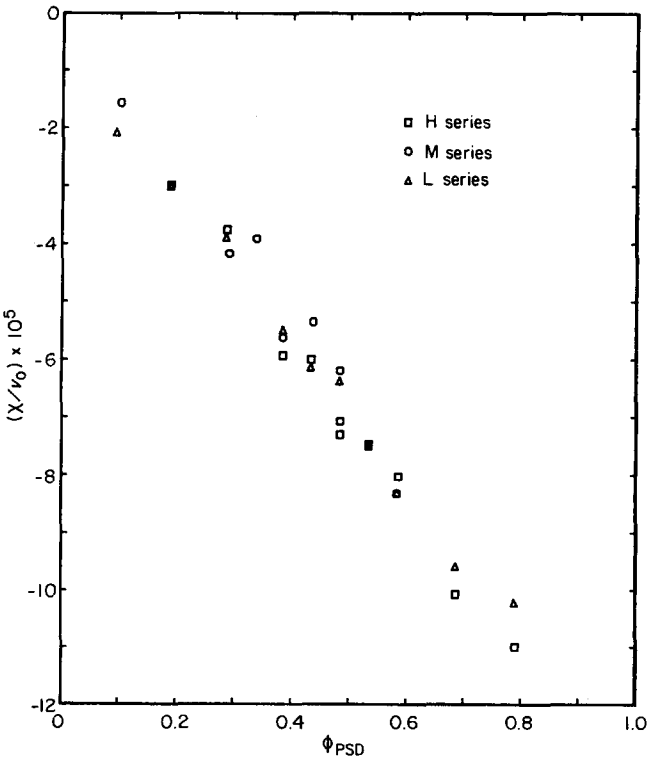

Figure 7 Interaction parameter χ/v_0 vs. ϕ_{PSD} for all three series of samples at 130°C

two different functional forms:

$$\frac{\chi}{v_0} = A + B\phi + \frac{C + D\phi}{T} + E\phi^2 \tag{25}$$

and

$$\frac{\chi}{v_0} = A + \frac{B\phi^2}{(1 + C\phi^2)^{1/2}} + \frac{D + E\phi}{T} \tag{26}$$

We should point out that both equations (25) and (26) are empirical formulae; we do not think we can attach any theoretical significance to them at this time. The χ/v_0 data for the L series and the best-fitted curves are shown in *Figure 8*.

In *Figure 9*, $\chi_{\mu 1}/v_0$, $\chi_{\mu 2}/v_0$, χ_s/v_0 and χ_F/v_0 are displayed against ϕ_{PSD} for the H series at $T = 100°C$. Using the model equations (25) and (26) we have tried the analysis of L, M and H series separately as well as by combining results from L and H series together. The M series sample was prepared without any antioxidant. There was discolouring of the sample after it was heated at high temperature (100–150°C) for about one day in the SANS experiment. Therefore, we have chosen to analyse the χ/v_0 values from the H series and L series samples together. The best-fitted parameters for both equations (25) and (26) are listed in *Table 2*. The calculated free-energy curves at several temperatures for the H series are shown in *Figure 10* together with the corresponding spinodal curve and measured spinodal temperatures.

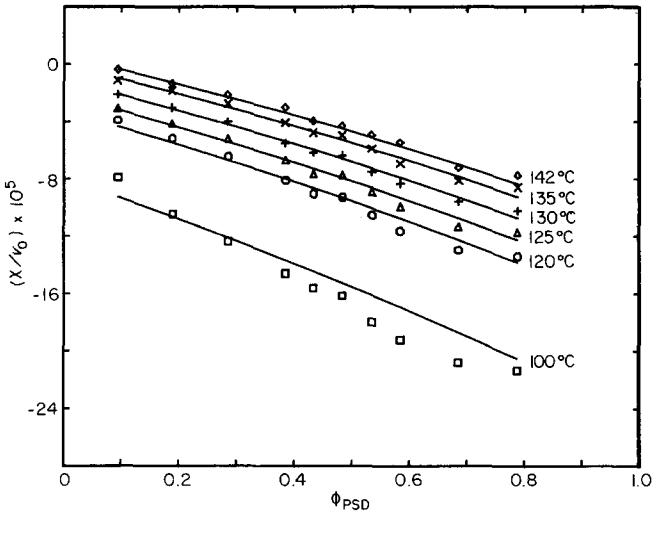

Figure 8 Interaction parameter χ/v_0 of the H series sample plotted against ϕ for various temperatures as shown in the figure. Full curves are non-linear least-square fit to the data according to equation (25)

With the knowledge of χ_F as a function of T and ϕ, the cloud-point curve can also be generated. Equations (27) and (28) can be used to calculate the spinodal and critical point respectively for a polydisperse system, where N_w and N_z are the weight-average and z-average degrees of polymerization, respectively:

$$2\chi = 2\chi_F - 2(1-2\phi)\frac{\partial \chi_F}{\partial \phi} - \phi(1-\phi)\frac{\partial^2 \chi_F}{\partial \phi^2}$$

$$= \frac{v_0}{v_A N_{Aw} \phi} + \frac{v_0}{v_B N_{Bw}(1-\phi)} \tag{27}$$

$$-6\frac{\partial \chi_F}{\partial \phi} - 3(1-2\phi)\frac{\partial^2 \chi_F}{\partial \phi^2} + \phi(1-\phi)\frac{\partial^3 \chi_F}{\partial \phi^3} = \frac{v_0 N_{Az}}{N_{Aw}^2 \phi^2} - \frac{v_0 N_{Bz}}{N_{Bw}^2 (1-\phi)^2} \tag{28}$$

Calculation of the cloud point requires a numerical solution. This was carried out according to the procedure described in Appendix 1.

In *Figure 11*, the spinodal curves generated with molecular weights corresponding to the H, M and L series from the χ/v_0 values obtained from the analysis in the last section are displayed together with spinodal temperatures obtained experimentally. The consistency between calculated and experimental spinodal temperatures of H and L series are quite satisfactory despite the fact that the spinodal temperatures are very sensitive to the χ_F value. Fitted parameters by using data from H and L series together for equations (25) and (26) are also listed in *Table 2*. On the other hand, for the M series sample, measured spinodal temperatures are inconsistent with the L and H series. This is due to the small amount of degradation and/or crosslinking as mentioned before. We should point out that a very small experimental deviation in the sample preparation and handling such as moisture content, degradation and crosslinking could result in a

Table 2 Best-fitted parameters

	Model 1 (equation (25))				
Parameters	Series H	Series M	Series L	Series H+L	Series H+L[a]
A	8.368×10^{-4}	1.093×10^{-3}	8.121×10^{-4}	8.257×10^{-4}	8.714×10^{-4}
B	3.694×10^{-4}	-6.523×10^{-5}	9.663×10^{-4}	6.138×10^{-4}	4.749×10^{-4}
C	-3.420×10^{-1}	-4.368×10^{-1}	-3.338×10^{-1}	-3.339×10^{-1}	-3.543×10^{-1}
D	-1.899×10^{-1}	-4.895×10^{-2}	-4.097×10^{-1}	-2.806×10^{-1}	-2.461×10^{-1}
E	-2.662×10^{-1}	7.056×10^{-5}	-1.205×10^{-4}	-6.280×10^{-5}	0
	Model 2 (equation (26))				
Parameters	Series H	Series M	Series L	Series H+L	
A	8.367×10^{-4}	–	8.096×10^{-4}	8.237×10^{-4}	
B	3.426×10^{-3}	–	7.478×10^{-3}	5.092×10^{-3}	
C	8.927×10^{1}	–	6.854×10^{1}	7.407×10^{1}	
D	-3.35×10^{-1}	–	-3.155×10^{-1}	-3.264×10^{1}	
E	-2.018×10^{-1}	–	-4.427×10^{-1}	-3.029×10^{-1}	

[a] Best fit of non-linear least squares with E fixed at 0

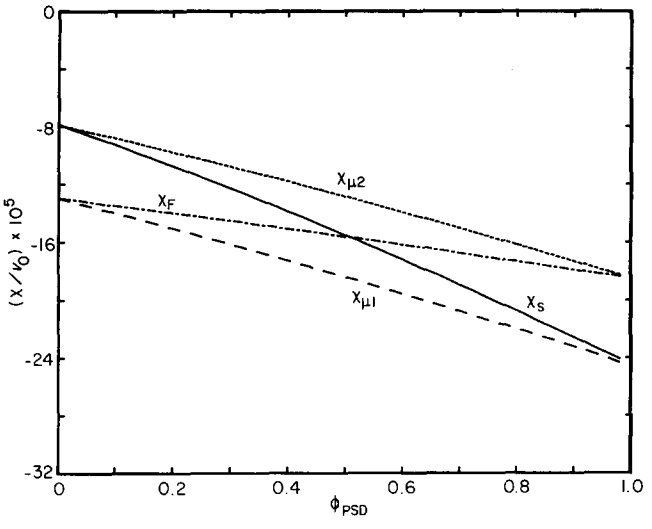

Figure 9 χ_S, $\chi_{\mu 1}$, $\chi_{\mu 2}$ and χ_F divided by v_0 obtained from the H series data and equation (25) at 100°C displayed as a function of ϕ_{PSD}

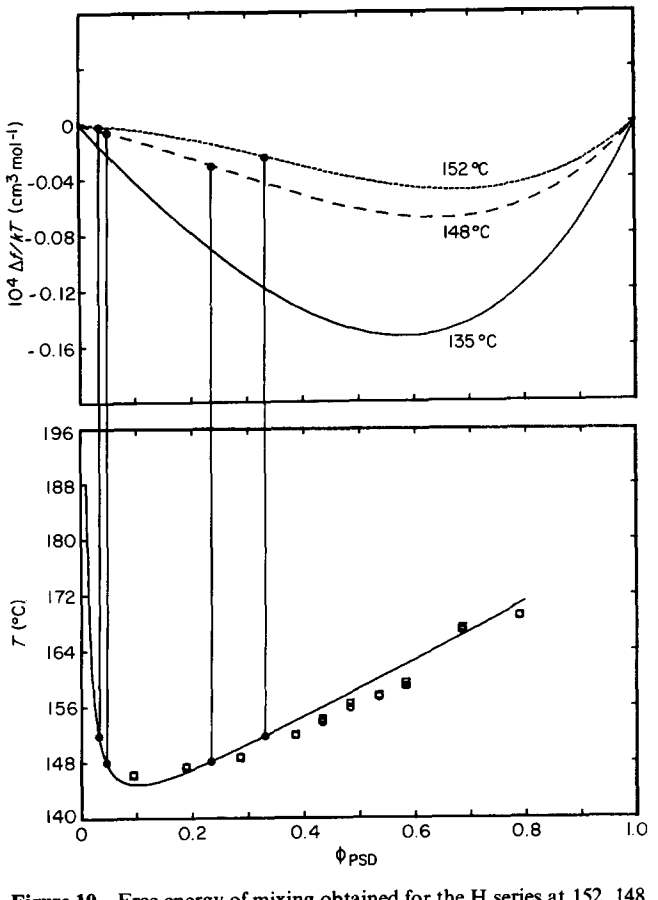

Figure 10 Free energy of mixing obtained for the H series at 152, 148 and 135°C (below critical temperature) plotted against ϕ_{PSD} in the upper part of the figure. The spinodal temperature line together with experimental data points (open circle and open square) are displayed in the lower part. The calculated spinodal points at 152°C and 148°C are also shown as full circles

fairly small χ change, but a very large shift in spinodal temperatures. This is obvious from equation (27) because of the small magnitude of entropic terms. Also shown in *Figure 11* are cloud-point curves generated according to Appendix 1.

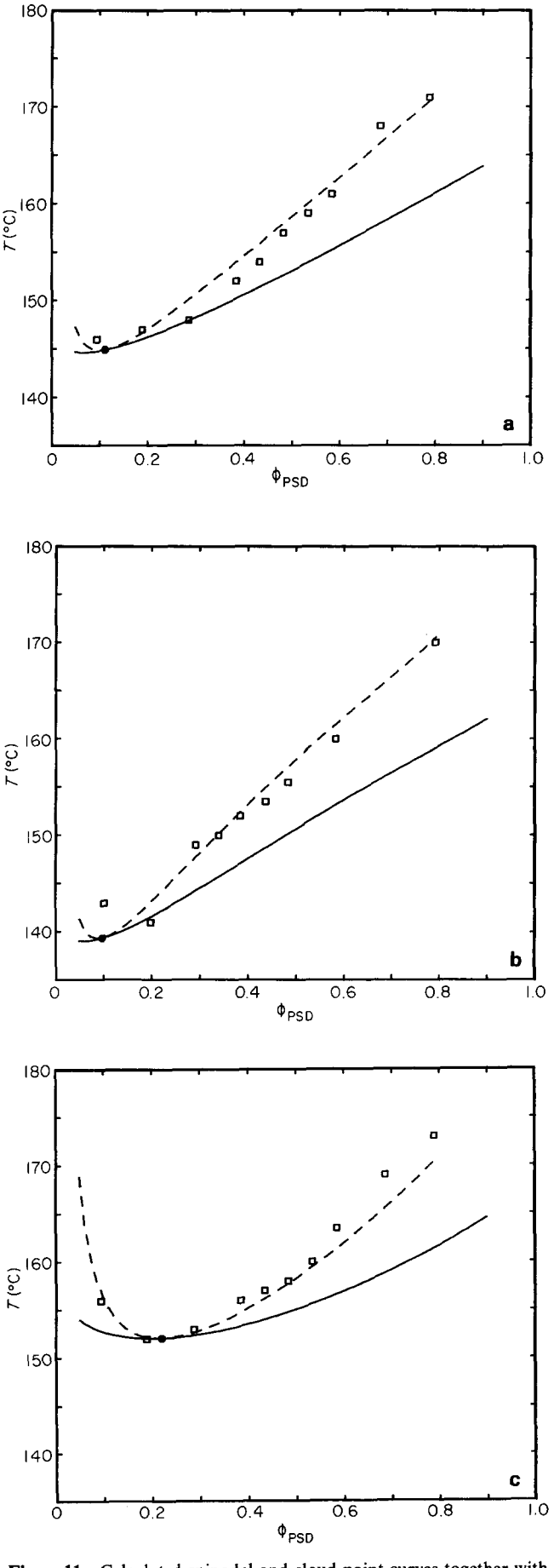

Figure 11 Calculated spinodal and cloud-point curves together with experimental data for (a) H series of samples, (b) M series of samples and (c) L series of samples: (□) spinodal from $S(0)$ and ξ; (– – –) spinodal from χ; (———) cloud point from χ; (●) critical point from χ

CONCLUSIONS

In this study we have measured χ/v_0 as a function of temperature and composition for three different molecular-weight combinations of PSD/PVME blends. The second derivative of free energy can be used directly in the kinetics studies of spinodal decomposition[20]. On the other hand, the binary interaction parameter χ_F can be obtained according to Sanchez' theory[9] and the free-energy function can be generated with an empirical functional form of the measured χ/v_0. Spinodal temperatures and cloud-point curves have been generated and compared with experimental values.

It is important to notice that small variations in experimental procedure could lead to a large change in measured spinodal temperatures which is not reflected in the small-magnitude change in χ/v_0. Nevertheless, one could still use the actually measured spinodal temperature in the equation $\partial^2 f/\partial\phi^2 = K(T^{-1} - T_s^{-1})$ for a given composition and obtain very good agreement with other measurements. For example, M series data can be superimposed with L and H series by using actually measured T_s in the above equation. In this study, possibly because of large molecular weights used in all three series, we do not observe an obvious molecular-weight dependence of χ_F.

ACKNOWLEDGEMENTS

The authors express sincere thanks to Drs Jeff Marqusee, Frank McCrackin and C. J. Glinka for their fruitful discussions, help in computer programming and SANS experiments.

REFERENCES

1 Paul, D. R. and Newman, S (Eds.), 'Polymer Blends', Vols. I and II, Academic Press, New York, 1978; Olabisi, O., Robeson, L. M. and Shaw, M. T. 'Polymer–Polymer Miscibility', Academic Press, New York, 1979
2 Herkt-Maetzky, C. and Schelton, J. *Phys. Rev. Lett.* 1983, **51**, 896
3 Yang, H., Shibayama, M., Stein, R. S. and Han, C. C. *Polym. Bull.* 1984, **12**, 7
4 Shibayama, M., Yang, H., Stein, R. S. and Han, C. C. *Macromolecules* 1985, **18**, 2179
5 Patterson, D., Bhattacharyya, S. N. and Picker, P. *Trans. Faraday Soc.* 1968, **64**, 648
6 Sanchez, I. C. and LaCombe, R. H. *J. Phys. Chem.* 1976, **80**, 2352; LaCombe, R. H. and Sanchez, I. C. *J. Phys. Chem.* 1976, **80**, 2568
7 Koningsveld, R., Kleintjens, L. A. and Schoffleers, H. M. *Pure Appl. Chem.* 1974, **39**, 1; Koningsveld, K. *Adv. Colloid Interface Sci.* 1968, **2**, 151
8 Muthukumar, M. *J. Chem. Phys.* 1986, **85**, 4722
9 Sanchez, I., private communication
10 de Gennes, P. G. *J. Physique* 1970, **31**, 235; 'Scaling Concepts in Polymer Physics', Cornell University Press, Ithaca, NY, 1979
11 Binder, K. *J. Chem. Phys.* 1983, **79**, 6387
12 Joanny, R. F. *J. Physique (A)* 1978, **11**, L117
13 de Gennes, P. G. *J. Physique Lett.* 1977, **38**, L441
14 Matsushita, Y. *et al. Polym. J.* 1982, **14**, 489
15 Bauer, B. J., Hanly, B. and Muroga, Y., to be published
16 Glinka, C. J. 'Neutron Scattering', AIP Conf. Proc. No. 89, Argonne National Lab., 1981, p. 395; Glinka, C. J., Rowe, J. M. and LaRock, J. G. *J. Appl. Crystallogr.* 1986, **19**, 427
17 Schwahn, D., Mortensen, K. and Yee-Madeira, H. *Phys. Rev. Lett.* 1987, **15**, 1544
18 Flory, P. J. 'Principles of Polymer Chemistry', Cornell University Press, Ithaca, NY, 1953
19 Koningsveld, R., Chermin, H. A. G. and Gordon, M. *Proc. R. Soc. Lond. (A)* 1970, **319**, 331
20 Han, C. C., Sato, T., Okada, M. and Wu, C. *Polym. Preprints (ACS)* 1987, **28(1)**, 358
21 Roe, R.-J. and Lu, L. *J. Polym. Sci., Polym. Phys. Edn.* 1985, **23**, 917
22 Bauer, B. J. *Polym. Eng. Sci.* 1985, **25**, 1081
23 Schultz, G. V. *Phys. Chem. Abt. (B)* 1985, **43**, 25, 1081; Zimm, B. H. *J. Chem. Phys.* 1948, **16**, 1099

APPENDIX 1

Roe[21] has calculated cloud-point curves for polymers with molecular-weight distributions, but χ was assumed to be independent of composition ϕ. In the following description, ϕ is the volume fraction of a component in a phase, N is the number of repeat units in a polymer, v is the volume fraction of a phase, χ is the interaction parameter and μ/RT is the chemical potential. The subscripts A or B refer to the two polymer types, 1 or 2 to the two phases, and i to a particular component (i.e. a particular degree of polymerization). The chemical potential of a polymer A in phase 1 is given in equation (A.1) and the chemical potential of polymer B in phase 1 is given in equation (A.2):

$$\frac{\mu_{Ai}}{RT} = \ln(\phi_{Ai}) - \left(1 - \frac{N_{Ai}}{N_1}\right) + N_{Ai}\left(\chi(1-\phi_{A1})^2 + \phi_{A1}(1-\phi_{A1})^2 \frac{\partial\chi}{\partial\phi_A}\right) \tag{A.1}$$

$$\frac{\mu_{Bi}}{RT} = \ln(\phi_{Bi}) - \left(1 - \frac{N_{Bi}}{N_1}\right) + N_{Bi}\left(\chi\phi_{A1}^2 - \phi_{A1}^2(1-\phi_{A1})\frac{\partial\chi}{\partial\phi_A}\right) \tag{A.2}$$

Parameter χ is an arbitrary function of ϕ and T and must be evaluated at the temperature and composition of interest. For simplicity the subscripts are neglected in this section. In equations (A.1) and (A.2) ϕ_{Ai} and ϕ_{Bi} are the volume fraction of species A_i and B_i in phase 1 respectively. This is equal to the volume of A_i or B_i divided by the phase volume v_1. At equilibrium the chemical potential of any polymer species is the same in both phases, and the amount of i in both phases at equilibrium is related. Equation (A.3) shows how polymer A will partition itself between the two phases:

$$P_{Ai1} = v_1 \exp\left[1 - \frac{N_{Ai}}{N_1} - N_{Ai}\left(\chi(1-\phi_{A1})^2 + \phi_{A1}(1-\phi_{A1})^2\frac{\partial\chi}{\partial\phi_A}\right)\right] \left\{v_1 \exp\left[1 - \frac{N_{Ai}}{N_1} - N_{Ai}\left(\chi(1-\phi_{A1})^2 + \phi_{A1}(1-\phi_{A1})^2\frac{\partial\chi}{\partial\phi_A}\right)\right] + v_2 \exp\left[1 - \frac{N_{Ai}}{N_2} - N_{Ai}\left(\chi\phi_{A1}^2 - \phi_{A1}^2(1-\phi_{A1})\frac{\partial\chi}{\partial\phi_A}\right)\right]\right\}^{-1}$$

$$P_{Ai2} = 1 - P_{Ai1} \tag{A.3}$$

P_{Ai1} is the fraction of component A_i partitioned into phase 1 and P_{Ai2} is the fraction partitioned into phase 2. In this way the partitioning of each component can be calculated and by summing all the partitioning as in equations (A.4) to (A.6), the phase volumes, compositions

and number-average degrees of polymerization can be calculated:

$$v_1 = v_A \int_0^\infty P_{A1} W_A(N)\, dN + v_B \int_0^\infty P_{B1} W(N)\, dN \quad (A.4)$$

$$\phi_1 = v_A \int_0^\infty P_{A1} W_A(N)\, dN / v_1 \quad (A.5)$$

$$\frac{1}{N_1} = \left(v_A \int_0^\infty \frac{P_{A1} W_A(N)}{N} dN + v_B \int_0^\infty \frac{P_{B1} W_B(N)}{N} dN \right) \Big/ v_1 \quad (A.6)$$

Here we have assumed that species A or B follows a continuous distribution function $W_A(N)$ or $W_B(N)$ respectively. N_1 is the number-average degree of polymerization of phase 1. A numerical solution can be found giving the equilibrium phase values; the numerical scheme has been described elsewhere[22].

The integrations of equations (A.4) to (A.6) cannot be solved in general for arbitrarily sized volumes of phases in equilibrium, but in the limit of one of the phases going to zero volume, which is the cloud point, the integrations can be carried out[21] for model distributions such as the Zimm–Schultz distribution[23]. On substituting the Zimm–Schultz distribution:

$$W(N) = \frac{(k/N_w)^k}{\Gamma(k)} N^{k-1} \exp(-Nk/N_w) \quad (A.7)$$

into equations (A.4) to (A.6), we can obtain (A.8) to (A.12):

$$v_1 = v_A \left(\frac{1}{1 - Q_A N_{wA}/k_A} \right)^{k_A} + v_B \left(\frac{1}{1 - Q_B N_{wB}/k_B} \right)^{k_B} \quad (A.8)$$

$$\phi_{1A} = v_A \left(\frac{1}{1 - Q_A N_{wA}/k_A} \right)^{k_A} \Big/ v_1 \quad (A.9)$$

$$\frac{1}{N_1} = \frac{v_A k_A}{(k_A - 1) N_{wA}} \left(\frac{1}{1 - Q_A N_{wA}/k_A} \right)^{k_A - 1} + \frac{v_B k_B}{(k_B - 1) N_{wB}} \left(\frac{1}{1 - Q_B N_{wB}/k_B} \right)^{k_B - 1} \quad (A.10)$$

$$Q_A = \frac{1}{N_1} - \frac{1}{N_2} - \chi[(1-\phi_{A1})^2 - (1-\phi_{A2})^2] - \frac{\partial \chi}{\partial \phi_A}[\phi_{1A}(1-\phi_{A1})^2 - \phi_{A2}(1-\phi_{A2})^2] \quad (A.11)$$

$$Q_B = \frac{1}{N_1} - \frac{1}{N_2} - \chi(\phi_{A1}^2 - \phi_{A2}^2) + \frac{\partial \chi}{\partial \phi_A}[\phi_{A1}^2(1-\phi_{A1}) - \phi_{A2}^2(1-\phi_{A2})] \quad (A.12)$$

Now the numerical solution is greatly simplified since numerical integrations are not necessary. The parameter k is related to the polydispersity, $k = 1/(1 - x_n/x_w)$.

Now there are only three variables, the volume, composition and number-average degree of polymerization of one of the phases. The volume, composition and degree of polymerization of the other phase can be calculated by conservation of mass. It is a simple task to find the values of the three variables that satisfy equations (A.8) to (A.10) by use of the Newton–Raphson method[22].

APPENDIX 2

Experimental values of ξ, $S(0)$ and χ/v_0 from SANS measurements are given in tabular form here.

MW	Designation	ϕ_{PSD}	T (°C)	χ/v_0 ($\times 10^5$)	ξ (Å)	$S(0)$	T_s (°C)
H	10/90	0.0951	100.0	−7.88	54.3	33.8	146.0
			120.0	−3.89	73.6	61.2	
			125.0	−3.06	80.5	73.5	
			130.0	−2.08	92.3	96.5	
			135.0	−1.11	111.1	140.1	
			138.0	−0.539	136.3	209.7	
			138.0	−0.365	137.1	214.4	
			142.0	0.306	189.9	410.7	
	20/80	0.1897	100.0	−10.45	35.9	27.3	147.0
			120.0	−5.16	50.8	52.7	
			125.0	−4.11	56.4	64.6	
			130.0	−3.00	64.6	84.8	
			135.0	−1.82	79.4	126.8	
			138.0	−1.32	89.4	160.9	
			142.0	−0.621	113.3	256.4	
			144.0	−0.206	140.6	396.6	
			146.0	0.222	216.3	907.8	
			148.0	0.526	748.0	11053.0	

(*continued on next page*)

MW	Designation	ϕ_{PSD}	*T* (°C)	χ/v_0 ($\times 10^5$)	ξ (Å)	*S*(0)	T_s (°C)
	30/70	0.2864	100.0	−12.36	27.6	23.6	148.0
			120.0	−6.44	38.2	44.1	
			125.0	−5.19	42.8	53.9	
			130.0	−3.98	48.3	68.8	
			135.0	−2.73	57.5	96.4	
			138.0	−2.11	64.3	120.4	
			142.0	−1.18	81.9	190.9	
			146.0	−0.362	118.8	398.1	
			148.0	−0.0177	168.2	799.7	
	40/60	0.3854	100.0	−14.57	22.5	20.2	152.0
			120.0	−8.09	30.7	35.8	
			125.0	−6.69	33.8	43.0	
			130.0	−5.49	37.0	51.8	
			135.0	−4.06	43.1	68.8	
			138.0	−2.98	49.9	91.4	
			142.0	−2.10	58.1	124.3	
			146.0	−1.19	74.3	199.9	
			148.0	−0.760	88.1	278.8	
			150.0	−0.301	116.9	484.8	
			152.0	0.113	203.4	1446.0	
	45/55	0.4338	100.0	−15.58	21.1	19.0	154.0
			120.0	−9.04	27.6	32.3	
			125.0	−7.66	30.3	37.9	
			130.0	−6.14	33.5	46.8	
			135.0	−4.77	38.2	59.4	
			138.0	−3.95	41.9	70.9	
			142.0	−3.02	47.6	90.0	
			144.0	−2.59	51.3	104.3	
			146.0	−1.70	61.5	150.3	
			148.0	−1.29	69.4	189.5	
			150.0	−0.813	83.4	270.6	
			152.0	−0.357	108.9	457.9	
			154.0	0.0991	199.3	1497.0	
	50/50	0.4837	100.0	−16.12	19.5	18.4	157.0
			120.0	−9.27	26.1	31.5	
			125.0	−7.73	29.0	37.6	
			130.0	−6.37	31.8	45.3	
			135.0	−4.96	36.2	57.4	
			138.0	−4.28	38.7	66.0	
			140.0	−3.70	42.0	75.5	
			144.0	−2.77	48.3	98.7	
			146.0	−2.29	52.3	117.2	
			148.0	−1.80	58.5	144.5	
			152.0	−0.872	79.3	260.2	
			154.0	−0.470	97.9	398.6	
			156.0	−0.0187	155.8	988.3	
	55/45	0.5349	100.0	−17.97	18.8	16.5	159.0
			120.0	−10.54	24.6	27.8	
			125.0	−8.91	27.1	32.8	
			130.0	−7.50	29.2	38.8	
			135.0	−5.88	33.1	48.9	
			138.0	−4.91	36.6	58.1	
			142.0	−3.83	41.1	73.4	
			146.0	−2.80	47.7	97.8	
			150.0	−1.88	56.8	139.8	
			154.0	−0.914	77.2	252.8	
			156.0	−0.491	96.2	392.0	
			158.0	0.164	261.0	2655.0	
	60/40	0.5840	100.0	−19.20	17.7	15.5	161.0
			120.0	−11.63	23.1	25.3	
			125.0	−9.94	25.1	29.5	
			130.0	−8.31	27.6	35.1	
			135.0	−6.91	30.3	41.9	
			138.0	−5.46	33.9	52.5	
			142.0	−4.38	37.8	64.7	
			146.0	−3.35	43.1	83.1	
			150.0	−2.38	50.6	113.7	
			154.0	−1.40	63.9	180.2	
			156.0	−0.986	73.3	239.0	
			158.0	−0.494	94.9	391.8	

(*continued on next page*)

MW	Designation	ϕ_{PSD}	T (°C)	χ/v_0 ($\times 10^5$)	ξ (Å)	$S(0)$	T_s (°C)
	70/30	0.6850	100.0	−20.78	17.2	14.3	168.0
			120.0	−12.95	22.3	22.8	
			125.0	−11.34	23.6	25.9	
			130.0	−9.59	26.0	30.5	
			135.0	−8.12	28.2	35.8	
			138.0	−7.22	29.7	40.1	
			142.0	−6.14	32.1	46.8	
			146.0	−5.15	35.0	55.4	
			150.0	−4.10	39.2	68.6	
			154.0	−3.22	43.9	85.9	
			158.0	−2.19	52.4	121.6	
			160.0	−1.75	57.8	147.6	
			162.0	−1.31	65.6	188.8	
			164.0	−0.875	76.6	259.0	
			166.0	−0.255	114.9	555.0	
	80/20	0.7889	100.0	−21.33	18.8	13.9	171.0
			120.0	−13.40	23.8	21.9	
			125.0	−11.72	25.5	25.0	
			130.0	−10.22	27.2	28.5	
			135.0	−8.57	29.6	33.8	
			138.0	−7.74	31.0	37.3	
			142.0	−6.87	32.8	41.8	
			146.0	−5.56	36.7	51.1	
			150.0	−4.53	40.3	61.8	
			154.0	−3.78	43.2	73.1	
			158.0	−2.69	51.1	99.2	
			162.0	−1.81	60.8	140.0	
			166.0	−0.837	82.3	255.2	
L	10/90	0.0942	120.0	−4.99	59.8	39.1	156.0
			130.0	−3.00	70.7	52.7	
			140.0	−0.595	92.3	90.9	
			145.0	−0.088	101.0	107.4	
			150.0	0.887	125.0	164.5	
			152.0	1.81	177.5	332.1	
			154.0	2.41	309.7	981.1	
	20/80	0.1901	120.0	−10.04	45.5	26.2	152.0
			130.0	−2.98	59.4	68.2	
			140.0	−1.08	78.0	119.6	
			145.0	−0.099	100.2	195.9	
			150.0	0.865	166.2	524.4	
			152.0	1.34	410.7	3122.0	
	30/70	0.2897	120.0	−6.39	35.7	40.6	153.0
			130.0	−3.76	45.4	62.9	
			140.0	−1.92	62.5	102.2	
			145.0	−0.769	80.5	167.5	
			150.0	0.360	135.9	450.0	
			152.0	0.950	398.9	3777.0	
	40/60	0.3850	120.0	−14.30	29.6	19.9	156.0
			130.0	−5.93	35.6	44.4	
			140.0	−3.47	47.0	69.8	
			145.0	−2.46	55.7	91.1	
			150.0	−0.992	69.6	163.8	
			152.0	0.063	107.6	384.1	
			154.0	0.534	171.9	960.7	
	45/55	0.4348	120.0	−8.57	27.3	32.2	157.0
			130.0	−6.00	32.1	44.4	
			140.0	−3.65	40.6	67.7	
			145.0	−2.48	47.7	91.9	
			150.0	−1.43	58.5	135.7	
			152.0	−0.347	82.2	263.9	
			154.0	0.096	105.9	431.4	
			156.0	0.629	226.1	1824.0	
	50/50	0.4848	120.0	−10.39	26.2	27.3	158.0
			120.0	−9.96	24.6	28.1	
			130.0	−7.07	31.3	38.5	
			130.0	−7.31	28.5	37.3	
			140.0	−4.22	39.8	60.5	
			140.0	−4.57	36.1	56.6	
			140.0	−4.22	36.9	60.5	
			145.0	−2.88	46.6	82.8	
			150.0	−2.19	52.1	102.7	
			152.0	−0.914	69.6	180.0	
			154.0	−0.427	82.7	253.8	
			156.0	0.120	114.5	470.6	

(*continued on next page*)

MW	Designation	ϕ_{PSD}	T (°C)	χ/v_0 ($\times 10^5$)	ξ (Å)	$S(0)$	T_s (°C)
	55/45	0.5347	120.0	−10.52	24.1	26.8	160.0
			130.0	−7.47	28.5	36.7	
			140.0	−4.55	36.0	56.9	
			145.0	−3.22	41.8	76.0	
			150.0	−2.03	50.4	108.9	
			152.0	−1.36	57.8	143.2	
			154.0	−0.955	64.6	177.6	
			156.0	−0.511	75.6	240.6	
			158.0	−0.0044	90.1	403.9	
	60/40	0.5862	120.0	−21.16	22.4	13.8	163.5
			130.0	−8.03	28.1	34.4	
			140.0	−5.89	32.3	45.5	
			145.0	−4.46	36.6	58.0	
			150.0	−3.25	41.9	75.5	
			154.0	−2.23	53.1	101.4	
			154.0	−1.42	57.4	139.4	
			158.0	−1.15	67.6	159.6	
			158.0	−0.472	77.5	249.2	
			160.0	−0.555	83.7	233.1	
			160.0	0.26	129.0	630.2	
			162.0	0.109	123.8	479.2	
	70/30	0.6867	120.0	−13.12	22.5	21.7	169.0
			130.0	−10.07	25.6	27.8	
			140.0	−6.25	32.5	42.9	
			145.0	−4.92	36.3	52.9	
			150.0	−3.77	40.9	66.2	
			154.0	−3.25	43.6	74.7	
			158.0	−2.33	49.7	97.0	
			162.0	−1.22	62.5	150.6	
			164.0	−0.686	73.6	205.4	
	80/20	0.7899	120.0	−26.09	22.7	11.1	173.0
			130.0	−10.99	27.4	25.2	
			140.0	−7.71	31.5	34.8	
			145.0	−6.26	34.7	41.8	
			150.0	−4.83	39.0	52.2	
			154.0	−3.70	43.4	64.9	
			158.0	−3.21	46.0	72.6	
			162.0	−2.26	52.4	93.9	
			164.0	−1.86	56.3	107.2	
			166.0	−1.39	61.9	129.0	
			168.0	−0.873	70.4	165.7	
			170.0	−0.013	101.0	314.3	
M	10/90	0.1025	100.0	−7.96	59.4	31.4	143.0
			110.0	−6.26	64.3	38.2	
			120.0	−3.70	78.8	56.6	
			125.0	−2.77	86.4	68.4	
			130.0	−1.87	94.1	85.9	
			135.0	−0.207	132.4	164.2	
			140.0	0.331	161.5	232.3	
	20/80	0.1986	100.0	−10.66	37.4	25.8	141.0
			120.0	−3.62	65.8	65.1	
			125.0	−2.19	79.1	93.9	
			130.0	−1.20	93.6	136.2	
			135.0	−0.281	123.6	233.6	
			140.0	0.572	212.8	689.8	
	30/70	0.2922	100.0	−14.49	28.3	19.7	149.0
			110.0	−10.55	33.2	26.5	
			120.0	−7.33	39.4	36.9	
			125.0	−5.44	44.8	48.1	
			130.0	−4.13	51.3	60.8	
			135.0	−2.69	61.3	85.5	
			140.0	−1.52	74.6	128.5	
			145.0	−0.180	115.2	299.4	
			150.0	0.617	263.4	1444.0	

(*continued on next page*)

MW	Designation	ϕ_{PSD}	T (°C)	χ/v_0 ($\times 10^5$)	ξ (Å)	$S(0)$	T_s (°C)
	35/65	0.3394	100.0	−11.80	26.6	23.9	150.0
			120.0	−6.49	36.1	41.6	
			125.0	−5.36	39.1	49.0	
			130.0	−3.93	44.9	63.8	
			135.0	−2.59	54.0	89.1	
			138.0	−1.91	60.2	111.8	
			140.0	−1.43	66.6	135.8	
			142.0	−1.06	72.3	163.5	
			143.0	−0.817	78.2	188.1	
			144.0	−0.599	84.4	217.6	
			145.0	−0.372	91.9	260.4	
			146.0	−0.128	104.1	329.9	
			147.0	−0.123	122.9	455.0	
			148.0	0.313	146.6	638.8	
			149.0	0.562	215.5	1350.3	
			150.0	0.640	271.6	2087.3	
	40/60	0.3851	120.0	−8.99	29.8	30.9	152.0
			125.0	−7.38	32.6	36.9	
			130.0	−5.62	37.3	47.2	
			135.0	−4.76	40.4	54.5	
			140.0	−2.59	52.5	89.8	
	45/55	0.4376	100.0	−13.15	24.1	21.7	153.5
			120.0	−7.97	31.8	34.5	
			125.0	−6.95	33.7	39.1	
			130.0	−5.38	37.5	49.0	
			135.0	−3.98	43.3	63.5	
			140.0	−2.60	50.3	87.2	
			143.0	−1.81	59.9	117.4	
			146.0	−1.20	68.1	153.9	
			149.0	−0.513	85.3	236.9	
			152.0	0.199	129.3	537.9	
	50/50	0.4843	100.0	−17.17	20.2	16.8	155.5
			110.0	−13.41	22.5	21.2	
			120.0	−9.82	26.6	28.4	
			125.0	−7.96	29.0	34.5	
			130.0	−6.14	33.1	43.6	
			135.0	−4.88	36.8	53.3	
			140.0	−3.65	41.4	68.2	
			145.0	−2.18	51.9	101.9	
			155.0	0.595	233.2	1739.3	
	60/40	0.5838	100.0	−17.29	19.4	16.6	160.0
			110.0	−13.81	22.4	20.6	
			120.0	−11.39	24.5	24.6	
			125.0	−9.93	26.1	27.9	
			130.0	−8.38	28.0	32.7	
			135.0	−6.35	31.8	41.9	
			140.0	−4.95	35.5	52.1	
			145.0	−3.47	41.9	69.9	
			150.0	−2.14	50.4	101.2	
			155.0	−0.873	66.7	176.4	
	80/20	0.7925	110.0	−15.58	21.3	17.8	170.0
			120.0	−11.29	24.6	23.8	
			125.0	−10.27	25.8	25.9	
			130.0	−8.68	28.0	30.0	
			135.0	−8.09	28.8	31.9	
			140.0	−6.49	31.9	38.3	
			145.0	−5.02	34.9	47.1	
			150.0	−3.69	40.0	59.4	
			155.0	−2.53	45.5	77.2	
			160.0	−1.69	51.1	98.2	
			165.0	−0.412	68.1	168.7	